Time-dependent density functional theory for quantum transport

Xiao Zheng, GuanHua Chen, Yan Mo, SiuKong Koo, Heng Tian, ChiYung Yam, and YiJing Yan

Citation: The Journal of Chemical Physics **133**, 114101 (2010); doi: 10.1063/1.3475566
View online: http://dx.doi.org/10.1063/1.3475566
View Table of Contents: http://scitation.aip.org/content/aip/journal/jcp/133/11?ver=pdfcov
Published by the AIP Publishing

Time-dependent density functional theory for quantum transport

Xiao Zheng,[1,2] GuanHua Chen,[2,3,4,a)] Yan Mo,[1,2,5] SiuKong Koo,[2] Heng Tian,[2] ChiYung Yam,[2] and YiJing Yan[1,b)]
[1]*Department of Chemistry, The Hong Kong University of Science and Technology, Hong Kong*
[2]*Department of Chemistry, The University of Hong Kong, Hong Kong*
[3]*Department of Physics, The University of Hong Kong, Hong Kong*
[4]*Centre for Theoretical and Computational Physics, The University of Hong Kong, Hong Kong*
[5]*Department of Applied Chemistry, National Chiao Tung University, Hsinchu 30050, Taiwan*

(Received 1 May 2010; accepted 14 July 2010; published online 16 September 2010)

Based on our earlier works [X. Zheng *et al.*, Phys. Rev. B **75**, 195127 (2007); J. S. Jin *et al.*, J. Chem. Phys. **128**, 234703 (2008)], we propose a rigorous and numerically convenient approach to simulate time-dependent quantum transport from first-principles. The proposed approach combines time-dependent density functional theory with quantum dissipation theory, and results in a useful tool for studying transient dynamics of electronic systems. Within the proposed exact theoretical framework, we construct a number of practical schemes for simulating realistic systems such as nanoscopic electronic devices. Computational cost of each scheme is analyzed, with the expected level of accuracy discussed. As a demonstration, a simulation based on the adiabatic wide-band limit approximation scheme is carried out to characterize the transient current response of a carbon nanotube based electronic device under time-dependent external voltages. © *2010 American Institute of Physics*. [doi:10.1063/1.3475566]

I. INTRODUCTION

The combined density functional theory (DFT) and nonequilibrium Green's function (NEGF) approach has been widely employed to simulate steady state quantum electron transport through molecular junctions and other nanoscopic structures. In practice, DFT introduces an effective single-electron reference system, on which NEGF analysis for steady current and electron occupation can be worked out. However, in principle, it remains obscure how the conventional DFT for ground/equilibrium state of isolated systems can provide a rigorous framework for quantum transport, as electron transport is intrinsically a dynamic process.

Time-dependent density functional theory (TDDFT) (Ref. 1) has been developed to study quantum transport phenomena.[2–10] As a formally rigorous and numerically tractable approach, TDDFT promises real-time simulations on ultrafast electron transport through realistic electronic devices or structures. In early attempts, finite source-device-drain systems were treated by the conventional TDDFT for isolated systems.[11–13] Since the source and drain were treated as finite, the results were not directly transferable to realistic devices coupled to bulk electrodes. By employing the NEGF approach and a partition-free scheme, Stefanucci and Almbladh[2] have derived the exact equations of motion for the two-time Green's functions within TDDFT framework. They and their co-workers have further proposed a practical scheme in which the electronic wavefunction propagates in time domain that subject to open boundaries.[3] The resulting numerical method has been tested on model systems. However, its applicability to realistic electronic devices remains unexploited.

Based on a reduced single-electron density matrix (RSDM) based formulation,[14,15] we have proposed a rigorous TDDFT approach for open electronic systems.[4,5] We have also developed an accurate numerical scheme,[6] based on a closed equation of motion (EOM) for the Kohn–Sham (KS) RSDM. Our RSDM based TDDFT-EOM has been combined with the Keldysh's NEGF formalism, the resulting TDDFT-NEGF-EOM approach has been applied successfully to exploit transient electronic dynamics in realistic molecular electronic devices.[6] One of the recent applications of the TDDFT-NEGF-EOM method was a simulation on the ultrafast transient current through a carbon nanotube based electronic device. It was found that the dynamic electronic response of the device can be mapped onto an equivalent classical electric circuit,[7,16] which would be useful for future design of functional devices.

Our previous simulations on realistic nanoelectronic devices[6,7] have demonstrated the numerical feasibility of our TDDFT-NEGF-EOM approach for open systems, while its accuracy is largely determined by the quality of approximated exchange-correlation (XC) functional which accounts for the many-particle effects, and that of dissipation functional which characterizes the dissipative interactions between the electronic device and electrodes. In our previous simulations, we employed the adiabatic local density approximation[17] (ALDA) for the XC functional and the adiabatic wide-band limit[6] (AWBL) approximation for the dissipation functional. Despite the success, the ALDA approximation is expected to become inadequate for addressing transient dynamics of open electronic systems in circum-

[a)]Electronic mail: ghc@everest.hku.hk.
[b)]Electronic mail: yyan@ust.hk.

stances where electron correlations dominate. Moreover, the frequency dispersion part of the XC potential is completely missing from an adiabatic XC functional such as ALDA,[18] which may lead to loss of crucial transient features in the electronic dynamics. The AWBL approximation for dissipation functional may lead to nontrivial errors for electrodes of finite bandwidths and strongly inhomogeneous energy bands, or when non-Markovian memory effects play a significant role (such as in multichannel conductors).

Several groups have shown that within TDDFT framework the steady state current can be formally expressed by Landauer–Büttiker formula, if the steady state can be reached.[2,6,10] This is important as the Landauer–Büttiker formula offers a convenient way to evaluate steady state current. However, in principle, it is the XC potential of TDDFT, which explicitly includes frequency-dependent component that should be used, instead of that of ground state DFT. In practice, the use of an adiabatic XC functional would lose all the memory of transient dynamics, and results in the same steady state current predicted by ground state DFT. Therefore, it is desirable to go beyond both the ALDA and AWBL approximations, and to develop more sophisticated XC and dissipation functionals for better characterization of transient electronic dynamics in quantum transport systems and structures.

Time-dependent quantum transport has been addressed from the perspective of open dissipative systems. Rossi *et al.*[19] have developed a single-electron density matrix based Bloch equation to simulate quantum-transport through mesoscopic devices. Burke *et al.*[9] have proposed a single-electron density matrix based master equation for a current-carrying electronic system with dissipation to a phonon bath. Weiss *et al.*[20] have proposed an iterative path-integral approach, which is numerically exact but computationally expensive. Myöhänen *et al.*[21] have extended the Kadanoff–Baym approach to open interacting systems,[22,23] where the roles of initial correlations and memory effects were highlighted. The simulation of transient current has also been attempted by many-body quantum master equation approaches.[24–28] Yan and coworkers have started from a master equation based second-order quantum dissipation theory (QDT), and derived an EOM for the RSDM within TDDFT framework,[8] where the bulk electrodes are treated as electron reservoirs. This was followed by the recent establishment of a formally exact QDT for the dynamics of an arbitrary non-Markovian dissipative systems interacting with bath surroundings.[10] The exact QDT is formulated in terms of hierarchical equations of motion (HEOM), and applied to solve time-dependent quantum transport problems.[29–32] The HEOM-QDT is intrinsically a nonperturbative method, and is constructed to resolve the combined effects of many-particle interaction, dissipative coupling strength, and memory time. The outstanding numerical accuracy and efficiency of HEOM-QDT approach to transient current response of interacting electronic systems under arbitrary time-dependent voltage has been demonstrated in previous works.[30–32]

In this work, we aim at unifying our TDDFT-NEGF-EOM approach for open systems with the HEOM-QDT to establish a TDDFT-NEGF-HEOM method, which is formally exact and numerically efficient. With the TDDFT-NEGF-HEOM approach, the dissipation functional readily goes beyond the AWBL approximation, resulting in systematic improvement on the simulated transient electronic dynamics. Moreover, the TDDFT-NEGF-HEOM approach is also applicable to devices operating at finite temperatures.

This paper is organized as follows. In Sec. II, we briefly review the TDDFT-NEGF-EOM formalism for open electronic systems, and introduce the TDDFT-HEOM formalism. The two formalisms are then combined and resulted in a unified TDDFT-NEGF-HEOM formalism. In Sec. III, we exploit formally exact computational schemes to calculate the dissipation functional with the TDDFT-NEGF-HEOM formalism. In Sec. IV, we propose three approximate schemes to reduce further the computational cost. In Sec. V, a numerical example is presented, with analysis on the computational efficiency. We summarize our results in Sec. VI.

II. DENSITY MATRIX BASED TIME-DEPENDENT DENSITY FUNCTIONAL THEORY FOR OPEN SYSTEMS

A. RSDM based TDDFT-EOM approach for isolated systems

We start with *ab initio* many-particle Hamiltonian of an *isolated* system containing N electrons

$$H(t)=\sum_{i=1}^{N}\left[-\frac{1}{2}\nabla_i^2+v(\boldsymbol{r}_i,t)\right]+\sum_{i<j}^{N}\frac{1}{\boldsymbol{r}_{ij}}, \tag{1}$$

where i and j run over all the N electrons, and $v(\boldsymbol{r}_i,t)$ is the external potential for the ith electron due to nuclei and other electrostatic sources. Atomic units are adopted here and throughout the rest of manuscript.

The Runge–Gross theorem[1] establishes the one-to-one correspondence between the external potential $v(\boldsymbol{r},t)$ and the time-dependent electron density function $\rho(\boldsymbol{r},t)$ of an isolated system. A time-dependent Kohn–Sham (TDKS) scheme has been proposed to solve $\rho(\boldsymbol{r},t)$, and hence all physical properties of the isolated system. The TDKS scheme follows the time evolution of an isolated reference system consisting of N noninteracting electrons. The Hamiltonian of the reference system is as follows:

$$\hat{H}(t)=\sum_{i=1}^{N}\hat{h}(\boldsymbol{r}_i,t)=\sum_{i=1}^{N}\left[-\frac{1}{2}\nabla_i^2+v_{\mathrm{eff}}(\boldsymbol{r}_i,t)\right], \tag{2}$$

where $v_{\mathrm{eff}}(\boldsymbol{r}_i,t)$ is the effective single-electron potential. A closed EOM has been derived for the KS RSDM $\boldsymbol{\sigma}$ of the isolated system[14,15]

$$i\dot{\boldsymbol{\sigma}}(t)=[\boldsymbol{h}(t),\boldsymbol{\sigma}(t)]. \tag{3}$$

Here, $\boldsymbol{h}(t)$ is the KS Fock matrix. Its matrix element is evaluated via $\boldsymbol{h}_{\mu\nu}(t)=\int\chi_\mu(\boldsymbol{r})\left[-\frac{1}{2}\nabla^2+v_{\mathrm{eff}}(\boldsymbol{r},t)\right]\chi_\nu(\boldsymbol{r})d\boldsymbol{r}$ in an atomic basis set $\{\chi_\mu(\boldsymbol{r})\}$. The square bracket on the right-hand side (RHS) of Eq. (3) denotes a commutator. The matrix element of $\boldsymbol{\sigma}$ is defined as $\boldsymbol{\sigma}_{\mu\nu}(t)\equiv\langle a_\nu^\dagger(t)a_\mu(t)\rangle$, where $a_\mu(t)$ and $a_\nu^\dagger(t)$ are Heisenberg annihilation and creation operators for an electron occupying atomic orbitals μ and ν at time t, respec-

tively. Fourier-transformed into frequency domain while considering linear response only, Eq. (3) leads to the conventional Casida's equation.[33]

B. RSDM based TDDFT-NEGF-EOM approach for open systems

In 2004, Fournais *et al.* have explored the real analyticity of electron density functions of many-electron systems.[34] They have proven that for a time-independent real physical system made of atoms and molecules, its electron density function is real analytic (except at nuclei), when the system is in its ground state or any one of its excited eigenstates. The real analyticity property immediately leads to the holographic theorem of *time-independent* systems: The ground-state electron density on any finite subsystem determines completely the electronic properties of the entire system.[4,35,36]

As for *time-dependent* systems, we have proven *holographic time-dependent electron density theorem*. Let $v(\boldsymbol{r},t)$ be the time-dependent external potential field on a finite physical system, $\rho(\boldsymbol{r},t_0)$ be its electron density function at a given time t_0, $\Phi(t_0)$ be the corresponding wavefunction, and $\rho_{\mathrm{D}}(\boldsymbol{r},t)$ the electron density function within any finite subspace D. If $\rho(\boldsymbol{r},t_0)$ is the real analytic in $\boldsymbol{r}$-space and $v(\boldsymbol{r},t)$ is the real analytic in both $\boldsymbol{r}$ and t, there is a *one-to-one* correspondence between $\rho_{\mathrm{D}}(\boldsymbol{r},t)$ and $v(\boldsymbol{r},t)$; consequently, $\rho_{\mathrm{D}}(\boldsymbol{r},t)$ determines uniquely the full *ab initio* Hamiltonian, and thus, all electronic properties of the entire time-dependent physical system. In principle, all one needs to know is the electron density in a local subsystem.

The above theorem for time-dependent open electron systems plays an analogous role as Runge–Gross theorem for isolated systems. Here, we shall not repeat the proof for the above theorem (see Ref. 6), but clarify several critical issues associated with the theorem and its proof, as follows:

(i) The entire physical system has to be *finite* (no matter how large in practice), and the total number of electrons in the entire system, N, is known via initial state $\Phi(t_0)$. N together with external field $v(\boldsymbol{r},t)$ determine uniquely the Hamiltonian of entire system. One can properly treat dissipation in an overall finite system, as long as the recurrence time of the reservior is much longer than the characteristic dynamic time of the system of interest. For quantum transport through a nanodevice, the macroscopic but finite leads have orders of magnitude larger degrees of freedom than that of the nanodevice, and can thus be treated as the environment to the open system, the nanodevice.

(ii) The proof of *holographic time-independent electron density theorem* is based on the real analyticity of static electron density function $\rho(\boldsymbol{r})$ in $\boldsymbol{r}$-space (except for isolated points at nuclei, since the rest of $\boldsymbol{r}$-space is all connected). In contrast, the validity of time-dependent version of theorem does *not* require the time-dependent electron density function $\rho(\boldsymbol{r},t)$ be real analytic in $\boldsymbol{r}$-space except at $t=t_0$. Instead, it requires the external potential $v(\boldsymbol{r},t)$ to be real analytic in space-time (after initial time), which is indeed the case in any realistic scenario. It is important to emphasize that the real analyticity property is utilized only to establish the *formal* one-to-one mapping between $\rho_{\mathrm{D}}(\boldsymbol{r},t)$ and $v(\boldsymbol{r},t)$. However, analytic continuation is expected to be numerically extremely difficult for either potential or density from within a subspace to its outside. Therefore, in practice it is desirable to seek for more convenient ways to exploit the explicit or implicit dependence of physical quantities on $\rho_{\mathrm{D}}(\boldsymbol{r},t)$.

(iii) For time-dependent systems, the real analyticity of $v(\boldsymbol{r},t)$ ensures that any change in external field at any place (at any finite distance away from subsystem D) will immediately modify the local external field $v_{\mathrm{D}}(\boldsymbol{r},t)$, and $v_{\mathrm{D}}(\boldsymbol{r},t)$ will invoke instantaneous local response in electron density $\rho_{\mathrm{D}}(\boldsymbol{r},t)$. Therefore, the above theorem guarantees that, in principle, $\rho_{\mathrm{D}}(\boldsymbol{r},t)$ reflects instantaneously any change in $v(\boldsymbol{r},t)$ at anywhere in $\boldsymbol{r}$-space. One could consider a practical example, in which the position of a nucleus far from D is displaced from t_0. This remote perturbation immediately changes the local electrostatic field inside D through long-range Coulomb interaction, and results in instantaneous response of $\rho_{\mathrm{D}}(\boldsymbol{r},t)$.

(iv) In analogy to Runge–Gross theorem[1] for isolated systems, holographic time-dependent electron density theorem involves explicitly a well-defined initial state $\Phi(t_0)$ for every system under study. Further remarks on initial-state dependence will be given after Eq. (10).

(v) Holographic time-dependent electron density theorem applies to the same phenomena and/or properties as those intended by Runge–Gross theorem, i.e., where electron density, in principle, provides the *minimal* amount of information necessary for establishing a one-to-one mapping with the scalar external field. This is true when the interaction between electrons and magnetic field is negligible. However, in the presence of an appreciable magnetic field, electron density alone becomes insufficient to determine the system properties.[37] In such cases, extra system information, the current density, is needed.[37] The above theorem for TDDFT should be generalized into the framework of time-dependent current-density functional theory.[37–39]

(vi) Due to the formal analogy between the time-dependent holographic electron density theorem and Runge–Gross theorem, we can define an action integral functional, $A[\rho_{\mathrm{D}}(\boldsymbol{r},t)]$, in a similar fashion as in the original paper of Runge and Gross (Ref. 1), i.e.,

$$A[\rho_{\mathrm{D}}] = \int_{t_0}^{t_1} dt \langle \Psi[\rho_{\mathrm{D}}] | i\,\partial/\partial t - H(t) | \Psi[\rho_{\mathrm{D}}] \rangle$$

$$= B[\rho_{\mathrm{D}}] - \int_{t_0}^{t_1} dt \int d\boldsymbol{r} \rho[\boldsymbol{r},t;\rho_{\mathrm{D}}] v(\boldsymbol{r},t). \qquad (4)$$

This is formally analogous to Eq. (10) in Ref. 1, so that $B[\rho_{\mathrm{D}}]$ is a universal functional of electron density

within subsystem D from its construction. This can be understood by noting that in addition to the wavefunction $\Psi[\rho_D]$, the electron density of the entire system is also completely determined by ρ_D, based on the holographic theorem ($\rho(\boldsymbol{r},t)=\rho[\boldsymbol{r},t;\rho_D]$). In this sense, in principle, we can also construct universal functionals such as $S[\rho_D]$ and $A_{xc}[\rho_D]$ in the same fashion as in Ref. 1, for the entire system. Therefore, in our TDDFT-HEOM approach the dependence of Kohn–Sham effective potential on $\rho_D(\boldsymbol{r},t)$ is also universal under any external field. Note that the causality paradox of TDDFT has been resolved.[40–42]

Based on the above theorem, we have developed a formally exact TDDFT-EOM formalism for open electronic systems. We consider coherent time-dependent quantum transport through a realistic electronic device. The entire system consists of bulk electrodes and the device region, where electron-electron scattering events mainly take place. For instance, in a two-terminal setup, the device region (D), left electrode (L), and right electrode (R) form the entire system. The region D is thus the open electronic system of primary interest.

Expanded in an atomic orbital basis set, the RSDM $\boldsymbol{\sigma}$ of entire system can be partitioned into a number of blocks, among which $\boldsymbol{\sigma}_\alpha$ and $\boldsymbol{\sigma}_D$ are the diagonal blocks corresponding to the electrode α (α=L or R) and the device region D, respectively; and $\boldsymbol{\sigma}_{\alpha D}=\boldsymbol{\sigma}_{D\alpha}^\dagger$ representing the off-diagonal block between the electrode α and the region D. The KS Fock matrix $\boldsymbol{h}$ can be partitioned in a similar fashion.

To obtain the reduced electronic dynamics of the device, we focus on the EOM of $\boldsymbol{\sigma}_D$

$$i\dot{\boldsymbol{\sigma}}_D=[\boldsymbol{h}_D,\boldsymbol{\sigma}_D]-i\sum_\alpha \boldsymbol{Q}_\alpha(t). \tag{5}$$

Here, $\boldsymbol{Q}_\alpha$ is the dissipation term due to the electrode α

$$\boldsymbol{Q}_\alpha(t)=i(\boldsymbol{h}_{D\alpha}\boldsymbol{\sigma}_{\alpha D}-\boldsymbol{\sigma}_{D\alpha}\boldsymbol{h}_{\alpha D}). \tag{6}$$

At first glance Eq. (5) seems not closed. However, based on holographic time-dependent electron density theorem, all physical quantities are explicit or implicit functionals of the electron density of the system D, $\rho_D(\boldsymbol{r},t)$, and so is $\boldsymbol{Q}_\alpha(t)$. Therefore, Eq. (5) can be cast into a formally closed form

$$i\dot{\boldsymbol{\sigma}}_D=[\boldsymbol{h}_D[t;\rho_D(\boldsymbol{r},t)],\boldsymbol{\sigma}_D]-i\sum_\alpha \boldsymbol{Q}_\alpha[t;\rho_D(\boldsymbol{r},t)], \tag{7}$$

by noting that $\rho_D(\boldsymbol{r},t)$ is the diagonal content of $\boldsymbol{\sigma}_D(t)$ in $\boldsymbol{r}$-space. Equation (7) is the heart of RSDM based TDDFT-EOM approach. The transient electric current through the interface S_α (the cross section separating region D from the electrode α) can be evaluated via

$$J_\alpha(t)=-\int_\alpha d\boldsymbol{r}\frac{\partial}{\partial t}\rho(\boldsymbol{r},t)=-\mathrm{tr}[\boldsymbol{Q}_\alpha(t)]. \tag{8}$$

In practice, conventional local or semilocal density approximation for XC potential can be adopted to construct the KS Fock matrix $\boldsymbol{h}_D[t;\rho_D(\boldsymbol{r},t)]$. The challenge now is to construct a formally exact and numerically accessible expression for $\boldsymbol{Q}_\alpha[t;\rho_D(\boldsymbol{r},t)]$.[10] Based on the Keldysh NEGF formalism, we have[6]

$$\boldsymbol{Q}_\alpha(t)=\boldsymbol{Q}_\alpha^0(t)-\int_{t_0}^t d\tau\left[\boldsymbol{G}_D^r(t,\tau)\boldsymbol{\Sigma}_\alpha^<(\tau,t)+\boldsymbol{G}_D^<(t,\tau)\boldsymbol{\Sigma}_\alpha^a(\tau,t)\right]+\mathrm{H.c.}, \tag{9}$$

at $t\geq t_0$. Here, t_0 is a time instant before the switch-on of external voltage, i.e., at time t_0 the entire system (including D and α) is fully connected and in its ground state. $\boldsymbol{G}_D$ and $\boldsymbol{\Sigma}_\alpha$ are the nonequilibrium Green's functions and self-energies associated with the corresponding noninteracting KS reference state; see Appendix B of Ref. 6 for details. The term $\boldsymbol{Q}_\alpha^0(t)$ in Eq. (9) explicitly accounts for the initial coherence between D and α at t_0. Therefore, Eq. (9) conforms formally with the partition-free scheme of NEGF method developed by Cini.[43] It is thus obvious that the particular form of dissipation function $\boldsymbol{Q}_\alpha[t;\rho_D(\boldsymbol{r},t)]$ depends explicitly on initial system state at t_0, $\Phi(t_0)$.

For numerical convenience of practical applications, we further notice that the initial noninteracting KS reference state, $\Psi(t_0)$, can be mathematically related to a fictitious noninteracting state, $\tilde{\Psi}$, where D and α are decoupled and in their respective isolated ground states. $\Psi(t_0)$ can be reached asymptotically from $\tilde{\Psi}$ via time propagation by adiabatically turning on couplings between D and α.[6] Taking $\tilde{\Psi}$ as $\Psi(t\to-\infty)$, Eq. (9) is cast into

$$\boldsymbol{Q}_\alpha(t)=-\int_{-\infty}^t d\tau\left[\boldsymbol{G}_D^r(t,\tau)\boldsymbol{\Sigma}_\alpha^<(\tau,t)+\boldsymbol{G}_D^<(t,\tau)\boldsymbol{\Sigma}_\alpha^a(\tau,t)\right]+\mathrm{H.c.} \tag{10}$$

The particular form of $\boldsymbol{Q}_\alpha(t)$ in Eq. (10) corresponds to the same initial physical state $\Phi(t_0)$ as that in Eq. (9). This is verified by the fact that both expressions give the same $\boldsymbol{Q}_\alpha(t)$ at $t\geq t_0$. The RHS of Eq. (10) corresponds to the partitioned scheme developed by Caroli *et al.*[44] In other words, despite the different KS reference states, Eqs. (9) and (10) exploit the same physical scenario, and are mathematically equivalent at $t\geq t_0$. In practice, Eq. (10) is numerically more convenient, as $\boldsymbol{G}_D$ and $\boldsymbol{\Sigma}_\alpha$ are more readily evaluated based on the decoupled fictitious state $\tilde{\Psi}$.

Approximate schemes based on NEGF formalism have been proposed in Ref. 6. In the following we will show that the exact HEOM-QDT provides another viable option for the evaluation of $\boldsymbol{Q}_\alpha[t;\rho_D(\boldsymbol{r},t)]$. The resulting TDDFT-HEOM approach is expected to improve systematically the accuracy of first-principles simulation on time-dependent quantum transport through realistic electronic devices.

C. Hierarchical TDDFT for open electronic systems

Differing from the conventional QDTs which assume weak device-electrode couplings, the HEOM-QDT formalism is considered as nonperturbative.[8] We consider a reference noninteracting electronic system within the TDKS framework

$$\hat{H}_{\mathrm{T}} = \hat{H}_{\mathrm{D}} + \sum_{\alpha} (\hat{H}_{\alpha} + \hat{H}_{\alpha\mathrm{D}}). \tag{11}$$

Here, $\hat{H}_{\mathrm{D}}$ is the KS Hamiltonian matrix for the device D, $\hat{H}_{\alpha}$ is the KS Hamiltonian matrix for the electrode α, and $\hat{H}_{\alpha\mathrm{D}}$ is the KS Hamiltonian matrix for the interaction between D and α. They are expressed as follows in second-quantization:

$$\hat{H}_{\mathrm{D}} = \sum_{\mu\nu\in\mathrm{D}} \boldsymbol{h}_{\mu\nu} a_{\mu}^{\dagger} a_{\nu},$$

$$\hat{H}_{\alpha} = \sum_{k\in\alpha} \boldsymbol{\epsilon}_{\alpha k} d_{\alpha k}^{\dagger} d_{\alpha k}, \tag{12}$$

$$\hat{H}_{\alpha\mathrm{D}} = \sum_{\mu\in\mathrm{D}} \sum_{k\in\alpha} \boldsymbol{t}_{\alpha k\mu} d_{\alpha k}^{\dagger} a_{\mu} + \mathrm{H.c.}$$

Here, $a_{\mu}^{\dagger}$ and a_{ν} are creation and annihilation operators for the reference electrons in the device D, respectively. $d_{\alpha k}^{\dagger}$ and $d_{\alpha k}$ are the creation and annihilation operators for the reference electrons in the electrode α, respectively. $\boldsymbol{h}_{\mu\nu} = \langle\mu|\hat{h}(\boldsymbol{r},t)|\nu\rangle = \int \chi_{\mu}(\boldsymbol{r})\left[-\frac{1}{2}\nabla^2 + v_{\mathrm{eff}}(\boldsymbol{r},t)\right]\chi_{\nu}(\boldsymbol{r})d\boldsymbol{r}$, $\boldsymbol{\epsilon}_{\alpha k} = \langle k_{\alpha}|\hat{h}(\boldsymbol{r},t)|k_{\alpha}\rangle$, and $\boldsymbol{t}_{\alpha k\mu} = \langle k_{\alpha}|\hat{h}(\boldsymbol{r},t)|\mu\rangle$. The EOM for the density matrix of the entire system (system plus electrodes) $\hat{\rho}_{\mathrm{T}}$ is

$$\begin{aligned}\dot{\hat{\rho}}_{\mathrm{T}} &= -i[\hat{H}_{\mathrm{T}}, \hat{\rho}_{\mathrm{T}}] \\ &= -i\left[\hat{H}_{\mathrm{D}} + \sum_{\alpha}\hat{H}_{\alpha}, \hat{\rho}_{\mathrm{T}}\right] - i\sum_{\alpha}\sum_{\mu\in\mathrm{D}}[f_{\alpha\mu}^{\dagger}a_{\mu} + a_{\mu}^{\dagger}f_{\alpha\mu}, \hat{\rho}_{\mathrm{T}}],\end{aligned} \tag{13}$$

with $f_{\alpha\mu} = \Sigma_k \boldsymbol{t}_{\alpha k\mu}^{*} d_{\alpha k}$ and $f_{\alpha\mu}^{\dagger} = \Sigma_k \boldsymbol{t}_{\alpha k\mu} d_{\alpha k}^{\dagger}$.

The TDDFT-EOM for the reduced system, Eq. (7), can be recovered. With the equality that $\boldsymbol{\sigma}_{\mu\nu}(t) = \mathrm{tr}_{\mathrm{T}}[a_{\nu}^{+}a_{\mu}\hat{\rho}_{\mathrm{T}}(t)]$, Eq. (13) leads to (cf. Ref. 45)

$$i\dot{\boldsymbol{\sigma}}_{\mathrm{D}} = [\boldsymbol{h}_{\mathrm{D}}, \boldsymbol{\sigma}_{\mathrm{D}}] - \sum_{\alpha}[\boldsymbol{\varphi}_{\alpha}(t) - \boldsymbol{\varphi}_{\alpha}^{\dagger}(t)], \tag{14}$$

where $\boldsymbol{\varphi}_{\alpha,\mu\nu}(t) \equiv \mathrm{tr}_{\mathrm{T}}[a_{\nu}^{+}f_{\alpha\mu}\hat{\rho}_{\mathrm{T}}(t)]$ and $\boldsymbol{\varphi}_{\alpha,\mu\nu}^{\dagger}(t) \equiv \mathrm{tr}_{\mathrm{T}}[f_{\alpha\nu}^{\dagger}a_{\mu}\hat{\rho}_{\mathrm{T}}(t)]$.

By comparing Eqs. (7) and (14), it is apparent the dissipation functional $\boldsymbol{Q}_{\alpha}[\rho_{\mathrm{D}}(\boldsymbol{r},t)]$ is directly associated with the first-tier auxiliary RSDM, $\boldsymbol{\varphi}_{\alpha}(t)$, as follows:

$$\boldsymbol{Q}_{\alpha}(t) = -i[\boldsymbol{\varphi}_{\alpha}(t) - \boldsymbol{\varphi}_{\alpha}^{\dagger}(t)] = -i\int d\epsilon[\boldsymbol{\varphi}_{\alpha}(\epsilon,t) - \boldsymbol{\varphi}_{\alpha}^{\dagger}(\epsilon,t)], \tag{15}$$

where $\boldsymbol{\varphi}_{\alpha}(t) = \int d\epsilon \boldsymbol{\varphi}_{\alpha}(\epsilon,t)$ and $\boldsymbol{\varphi}_{\alpha}^{\dagger}(t) = \int d\epsilon \boldsymbol{\varphi}_{\alpha}^{\dagger}(\epsilon,t)$.

A key feature of the exact HEOM-QDT is that for noninteracting systems, such as the TDKS reference system in the present case, the hierarchy terminates exactly at the second tier without any approximation.[10] The corresponding HEOM for the KS RSDM and its auxiliary counterparts have been derived in Ref. 10 as follows:

$$\begin{aligned}i\dot{\boldsymbol{\varphi}}_{\alpha}(\epsilon,t) &= [\boldsymbol{h}_{\mathrm{D}}(t) - \epsilon - \Delta_{\alpha}(t)]\boldsymbol{\varphi}_{\alpha}(\epsilon,t) \\ &\quad + [f_{\alpha}(\epsilon) - \boldsymbol{\sigma}_{\mathrm{D}}]\boldsymbol{\Lambda}_{\alpha}(\epsilon) + \sum_{\alpha'}\int d\epsilon' \boldsymbol{\varphi}_{\alpha,\alpha'}(\epsilon,\epsilon',t),\end{aligned} \tag{16}$$

$$\begin{aligned}i\dot{\boldsymbol{\varphi}}_{\alpha,\alpha'}(\epsilon,\epsilon',t) &= -[\epsilon + \Delta_{\alpha}(t) - \epsilon' - \Delta_{\alpha'}(t)]\boldsymbol{\varphi}_{\alpha,\alpha'} \\ &\quad + \boldsymbol{\Lambda}_{\alpha'}(\epsilon')\boldsymbol{\varphi}_{\alpha}(\epsilon,t) - \boldsymbol{\varphi}_{\alpha'}^{\dagger}(\epsilon',t)\boldsymbol{\Lambda}_{\alpha}(\epsilon).\end{aligned} \tag{17}$$

Here, $f_{\alpha}(\epsilon) = 1/[e^{\beta(\epsilon-\mu_{\alpha})}+1]$ is the Fermi distribution function for the electrode α, with β being the inverse temperature and μ_{α} the equilibrium Fermi energy; $\Delta_{\alpha}(t) = -V_{\alpha}(t)$ is the energy shift for all single-electron levels in electrode α due to the time-dependent voltage applied on α; $\boldsymbol{\Lambda}_{\alpha,\mu\nu}(\epsilon) \equiv \Sigma_{k\in\alpha}\delta(\epsilon-\epsilon_k)\boldsymbol{t}_{\alpha k\mu}^{*}\boldsymbol{t}_{\alpha k\nu}$, is the device-electrode coupling matrix.

Equations (14), (16), and (17) complete the TDDFT-HEOM formalism, which is formally exact and closed. The basic variables involved are the reduced single-electron quantities $\{\boldsymbol{\sigma}_{\mathrm{D}}(t), \boldsymbol{\varphi}_{\alpha}(\epsilon,t), \boldsymbol{\varphi}_{\alpha,\alpha'}(\epsilon,\epsilon',t)\}$.

D. TDDFT-NEGF-HEOM for quantum transport

We now make connection between the TDDFT-HEOM formalism to the RSDM based TDDFT-NEGF-EOM formalism. As shown in Ref. 45, the auxiliary RSDMs $\{\boldsymbol{\varphi}_{\alpha}(\epsilon,t), \boldsymbol{\varphi}_{\alpha,\alpha'}(\epsilon,\epsilon',t)\}$ can be expressed in terms of NEGF quantities as follows:[46]

$$\boldsymbol{\varphi}_{\alpha}(\epsilon,t) = i\int_{-\infty}^{t} d\tau\left[\boldsymbol{G}_{\mathrm{D}}^{<}(t,\tau)\boldsymbol{\Sigma}_{\alpha}^{>}(\tau,t;\epsilon) - \boldsymbol{G}_{\mathrm{D}}^{>}(t,\tau)\boldsymbol{\Sigma}_{\alpha}^{<}(\tau,t;\epsilon)\right], \tag{18}$$

$$\begin{aligned}&\boldsymbol{\varphi}_{\alpha,\alpha'}(\epsilon,\epsilon',t) \\ &= i\left[\int_{C} d\tau_1 \int_{C} d\tau_2 \boldsymbol{\Sigma}_{\alpha'}(t,\tau_1;\epsilon')\boldsymbol{G}_{\mathrm{D}}(\tau_1,\tau_2)\boldsymbol{\Sigma}_{\alpha}(\tau_2,t;\epsilon)\right]^{<}\end{aligned} \tag{19}$$

$$\begin{aligned}&= i\int_{-\infty}^{t} dt_1 \int_{-\infty}^{t} dt_2 \Big\{\Big[\boldsymbol{\Sigma}_{\alpha'}^{<}(t,t_1;\epsilon')\boldsymbol{G}_{\mathrm{D}}^{a}(t_1,t_2) \\ &\quad + \boldsymbol{\Sigma}_{\alpha'}^{r}(t,t_1;\epsilon')\boldsymbol{G}_{\mathrm{D}}^{<}(t_1,t_2)\Big]\boldsymbol{\Sigma}_{\alpha}^{>}(t_2,t;\epsilon) \\ &\quad - \left[\boldsymbol{\Sigma}_{\alpha'}^{r}(t,t_1;\epsilon')\boldsymbol{G}_{\mathrm{D}}^{>}(t_1,t_2) + \boldsymbol{\Sigma}_{\alpha'}^{>}(t,t_1;\epsilon')\boldsymbol{G}_{\mathrm{D}}^{a}(t_1,t_2)\right] \\ &\quad \times \boldsymbol{\Sigma}_{\alpha}^{<}(t_2,t;\epsilon)\Big\}.\end{aligned} \tag{20}$$

Here, $\boldsymbol{\Sigma}_{\alpha}^{x}(t,\tau;\epsilon)$ are frequency-dispersed self-energies ($x = r, a, <$ and $>$), which normalize to normal self-energies as $\int \boldsymbol{\Sigma}_{\alpha}^{x}(t,\tau;\epsilon)d\epsilon = \boldsymbol{\Sigma}_{\alpha}^{x}(t,\tau)$. It is straightforward to derive from Ref. 45 that

$$\mathbf{\Sigma}^x_\alpha(t,\tau;\epsilon) \equiv \exp\left[-i\int_\tau^t \Delta_\alpha(\zeta)d\zeta\right] e^{-i\epsilon(t-\tau)}\widetilde{\mathbf{\Sigma}}^x_\alpha(\epsilon)$$
$$= \exp\left[-i\int_\tau^t \Delta_\alpha(\zeta)d\zeta\right]\widetilde{\mathbf{\Sigma}}^x_\alpha(t-\tau;\epsilon). \quad (21)$$

This is formally analogous to normal self-energies with $\widetilde{\mathbf{\Sigma}}^x_\alpha$ being the ground/equilibrium-state quantities; see Ref. 45. The following EOM thus applies:

$$\frac{\partial}{\partial t}\mathbf{\Sigma}^x_\alpha(t,\tau;\epsilon) = -i[\Delta_\alpha(t)+\epsilon]\mathbf{\Sigma}^x_\alpha(t,\tau;\epsilon),$$
$$\frac{\partial}{\partial \tau}\mathbf{\Sigma}^x_\alpha(t,\tau;\epsilon) = i[\Delta_\alpha(\tau)+\epsilon]\mathbf{\Sigma}^x_\alpha(t,\tau;\epsilon). \quad (22)$$

Equations (14) and (16)–(20) are the central equations of the TDDFT-NEGF-HEOM formalism.

The stationary solution of TDDFT-NEGF-HEOM is related to the Landauer–Büttiker formula; see Ref. 45.

III. HIERARCHICAL EQUATIONS OF MOTION SCHEME FOR CALCULATION OF DISSIPATION FUNCTIONAL

A. Frequency dispersion scheme for TDDFT-HEOM

In order to numerically solve the TDDFT-HEOM for $\boldsymbol{Q}_\alpha(t)$, the integration over continuous function needs to be transformed into summation of discrete terms, i.e., $\int g(\epsilon)d\epsilon \rightarrow \Sigma_{k=1}^{N_k} w_k g(\epsilon_k)$. Here, ϵ_k and w_k are the kth *real* frequency grid and its associated weight ($0 \le w_k \le 1$ and $\Sigma_{k=1}^{N_k} w_k = 1$), respectively. We have thus

$$\boldsymbol{Q}_\alpha(t) = -i\sum_{k=1}^{N_k} w_k[\boldsymbol{\varphi}_{\alpha k}(t) - \boldsymbol{\varphi}^\dagger_{\alpha k}(t)]. \quad (23)$$

Equations (16) and (17) are recast into

$$i\dot{\boldsymbol{\varphi}}_{\alpha k} = [\boldsymbol{h}_{\mathrm{D}}(t) - \epsilon_k - \Delta_\alpha(t)]\boldsymbol{\varphi}_{\alpha k}(t) + [f_\alpha(\epsilon_k) - \boldsymbol{\sigma}_{\mathrm{D}}] \times \mathbf{\Lambda}_\alpha(\epsilon_k) + \sum_{\alpha'}\sum_{k'=1}^{N_k} w_{k'}\boldsymbol{\varphi}_{\alpha k,\alpha' k'}(t), \quad (24)$$

$$i\dot{\boldsymbol{\varphi}}_{\alpha k,\alpha' k'} = -[\epsilon_k + \Delta_\alpha(t) - \epsilon_{k'} - \Delta_{\alpha'}(t)]\boldsymbol{\varphi}_{\alpha k,\alpha' k'}(t) + \mathbf{\Lambda}_{\alpha'}(\epsilon_{k'})\boldsymbol{\varphi}_{\alpha k}(t) - \boldsymbol{\varphi}^\dagger_{\alpha' k'}(t)\mathbf{\Lambda}_\alpha(\epsilon_k). \quad (25)$$

Hereafter, we adopt abbreviations $\boldsymbol{\varphi}_{\alpha k}(t) \equiv \boldsymbol{\varphi}_\alpha(\epsilon_k,t)$ and $\boldsymbol{\varphi}_{\alpha k,\alpha' k'}(t) \equiv \boldsymbol{\varphi}_{\alpha,\alpha'}(\epsilon_k,\epsilon_{k'},t)$. In practice, application of quadrature rules, such as Gauss–Legendre quadrature, reduces significantly the number of frequency grids compared to an equidistant sampling. This frequency-dispersed TDDFT-HEOM scheme applies to both zero and finite temperatures. Next we propose several efficient schemes particularly designed for finite temperature cases.

B. Finite temperature schemes for TDDFT-NEGF-HEOM

The ground/equilibrium-state self-energies $\widetilde{\mathbf{\Sigma}}^x_\alpha(t)$ are usually exponentially decaying functions of time. Therefore, the following exponential expansion is attainable for $\widetilde{\mathbf{\Sigma}}^{<,>}_\alpha(\tau-t)$ at $t \ge \tau$

$$\widetilde{\mathbf{\Sigma}}^x_\alpha(\tau-t) \simeq \sum_{k=1}^{N_k} \boldsymbol{A}^x_{\alpha k}\exp[-\gamma_{\alpha k}(t-\tau)] \equiv \sum_{k=1}^{N_k}\widetilde{\mathbf{\Sigma}}^x_{\alpha k}(\tau-t), \quad (26)$$

for $x = <$ and $>$. $\gamma_{\alpha k}$ are c-numbers with $\mathrm{Re}(\gamma_{\alpha k}) > 0$. Moreover, the nonequilibrium self-energies $\mathbf{\Sigma}^x_{\alpha k}(\tau,t) \equiv e^{-i\int_t^\tau \Delta_\alpha(\zeta)d\zeta}\widetilde{\mathbf{\Sigma}}^x_{\alpha k}(\tau-t)$. Equation (15) becomes

$$\boldsymbol{Q}_\alpha(t) = -i\sum_{k=1}^{N_k}[\boldsymbol{\varphi}_{\alpha k}(t) - \boldsymbol{\varphi}^\dagger_{\alpha k}(t)]. \quad (27)$$

Here, $\boldsymbol{\varphi}_{\alpha k}(t)$ is given by the RHS of Eq. (18) with $\mathbf{\Sigma}^x_\alpha(\tau,t;\epsilon)$ replaced by $\mathbf{\Sigma}^x_{\alpha k}(\tau,t)$. The second-tier auxiliary RSDMs, $\boldsymbol{\varphi}_{\alpha k,\alpha' k'}(t)$, are formally obtained by substituting $\mathbf{\Sigma}^x_\alpha(t_2,t;\epsilon)$ with $\mathbf{\Sigma}^x_{\alpha k}(t_2,t)$ on the RHS of Eq. (20). EOM for $\boldsymbol{\varphi}_{\alpha k}$ and $\boldsymbol{\varphi}_{\alpha k,\alpha' k'}(t)$ now read

$$i\dot{\boldsymbol{\varphi}}_{\alpha k} = [\boldsymbol{h}_{\mathrm{D}}(t) - i\gamma_{\alpha k} - \Delta_\alpha(t)]\boldsymbol{\varphi}_{\alpha k}(t) + i[\boldsymbol{\sigma}_{\mathrm{D}}(t)\boldsymbol{A}^>_{\alpha k} + \bar{\boldsymbol{\sigma}}_{\mathrm{D}}(t)\boldsymbol{A}^<_{\alpha k}] + \sum_{\alpha'}\sum_{k'=1}^{N_k}\boldsymbol{\varphi}_{\alpha k,\alpha' k'}(t), \quad (28)$$

$$i\dot{\boldsymbol{\varphi}}_{\alpha k,\alpha' k'} = -[i\gamma_{\alpha k} + \Delta_\alpha(t) - i\gamma_{\alpha' k'} - \Delta_{\alpha'}(t)]\boldsymbol{\varphi}_{\alpha k,\alpha' k'} + i(\boldsymbol{A}^>_{\alpha' k'} - \boldsymbol{A}^<_{\alpha' k'})\boldsymbol{\varphi}_{\alpha k}(t) - i\boldsymbol{\varphi}^\dagger_{\alpha' k'}(t)(\boldsymbol{A}^>_{\alpha k} - \boldsymbol{A}^<_{\alpha k}). \quad (29)$$

Here, $\bar{\boldsymbol{\sigma}}_{\mathrm{D}} \equiv 1 - \boldsymbol{\sigma}_{\mathrm{D}}$ is the KS reduced single-hole density matrix. Equations (14), (28), and (29) constitute a reformulation of TDDFT-NEGF-HEOM formalism which is suitable for the numerical solution.

Apparently, the computational cost for solving the TDDFT-NEGF-HEOM is determined by the number of exponential functions N_k used to expand the lesser and greater self-energies. Next we propose three decomposition schemes to expand the self-energies as in Eq. (26).

1. Matsubara expansion decomposition scheme

The ground/equilibrium-state lesser and greater self-energies can be evaluated via

$$\widetilde{\mathbf{\Sigma}}^x_\alpha(\tau-t) = \varsigma_x i\int d\epsilon e^{i\epsilon(t-\tau)} f^{\varsigma_x}_\alpha(\epsilon)\mathbf{\Lambda}_\alpha(\epsilon), \quad (30)$$

for $t \ge \tau$. Here, $x = <$ or $>$, $\varsigma_< = +$ and $\varsigma_> = -$, and $f^+_\alpha(\epsilon) \equiv f_\alpha(\epsilon)$ and $f^-_\alpha(\epsilon) \equiv 1 - f_\alpha(\epsilon)$. Equation (30) states the fluctuation-dissipation theorem for electrode correlation functions. If the linewidth matrix $\mathbf{\Lambda}_\alpha(\epsilon)$ can be approximated via a multi-Lorentzian expansion as follows:

$$\mathbf{\Lambda}_\alpha(\epsilon) = \sum_{d=1}^{N_d}\frac{\eta_d}{(\epsilon-\Omega_d)^2 + W_d^2}\bar{\mathbf{\Lambda}}_{\alpha d}. \quad (31)$$

Here, η_d, Ω_d, and $W_d > 0$ are the coefficient, center, and width of dth fitting Lorentzian function; and $\bar{\mathbf{\Lambda}}_{\alpha d}$ is the corresponding frequency-independent linewidth matrix, respectively. The RHS of Eq. (30) is calculated via complex contour integral and residue theorem, for which analytic continuation of $\mathbf{\Lambda}_\alpha(\epsilon)$ and $f^\pm_\alpha(\epsilon)$ into complex plane is needed. $\mathbf{\Lambda}_\alpha(z)$ can be defined straightforwardly by replacing

ϵ with z on the RHS of Eq. (31), and $f_\alpha^{\pm}(\epsilon)$ is continued analytically to $f_\alpha^{\pm}(z)$ in the same fashion. At a finite temperature, the Matsubara expansion scheme for the Fermi function is as follows:

$$f_\alpha^{\mathfrak{s}}(z) \equiv \frac{1}{e^{\mathfrak{s}\beta(z-\mu_\alpha)}+1} \simeq \frac{1}{2} - \mathfrak{s}\frac{1}{\beta}\sum_{p=1}^{N_p}\left(\frac{1}{z+z_{\alpha p}} + \frac{1}{z-z_{\alpha p}}\right). \tag{32}$$

For the Matsubara expansion $z_{\alpha p}=\mu_\alpha+i\pi(2p-1)/\beta$.

With all the poles of $f_\alpha^{\mathfrak{s}}(z)$ and $\mathbf{\Lambda}_\alpha(z)$ in the upper-half complex plane accounted for, we arrive at the following exponential expansion of self-energies:

$$\tilde{\mathbf{\Sigma}}_\alpha^{x}(\tau-t) \simeq \sum_{d=1}^{N_d} \boldsymbol{A}_{\alpha d}^{x} e^{-\gamma_{\alpha d}(t-\tau)} + \sum_{p=1}^{N_p} \boldsymbol{B}_{\alpha p}^{x} e^{-\check{\gamma}_{\alpha p}(t-\tau)}, \tag{33}$$

with

$$\begin{aligned} \boldsymbol{A}_{\alpha d}^{x} &= i\frac{\mathfrak{s}_x\pi\eta_d}{W_d} f_\alpha^{\mathfrak{s}_x}(\Omega_d+iW_d)\bar{\mathbf{\Lambda}}_{\alpha d}, \\ \gamma_{\alpha d} &= W_d - i\Omega_d, \\ \boldsymbol{B}_{\alpha p}^{x} &= \frac{2\pi}{\beta}\mathbf{\Lambda}_\alpha(z_{\alpha p}), \\ \check{\gamma}_{\alpha p} &= -iz_{\alpha p} = -i\mu_\alpha + \frac{(2p-1)\pi}{\beta}. \end{aligned} \tag{34}$$

We then make connections between Eqs. (33) and (26). The total number of exponential terms is the sum of number of Lorentzian functions and number of Matsubara terms considered, i.e., $N_k=N_d+N_p$. In principle, $N_p\to+\infty$ is required to achieve an exact expansion for $\tilde{\mathbf{\Sigma}}_\alpha^{<,>}(\tau-t)$. In practice, a smallest possible N_p but guaranteeing an expected accuracy is desired. The value of N_p increases rapidly as the temperature is lowered.

2. Partial fractional decomposition scheme

A major disadvantage of the Matsubara expansion is the poor convergence at low temperature. Alternatively we may adopt the partial fractional decomposition (PFD) of Fermi function.[46] The PFD expansion is formally identical to Eq. (32), but with $z_{\alpha p}=\mu_\alpha+2\sqrt{\epsilon_p}/\beta$. Here, ϵ_p is the pth eigenvalue of the $N_p\times N_p$ matrix $\boldsymbol{Z}$ defined as follows:

$$\boldsymbol{Z}_{mn} = 2m(2m-1)\delta_{n,m+1} - 2N_p(2N_p-1)\delta_{m,N_p}, \tag{35}$$

with the constraint that $\mathrm{Im}(\sqrt{\epsilon_p})>0$.

With the same multi-Lorentzian expansion of Eq. (31), the self-energies are decomposed into exponential functions exactly as Eq. (33). The PFD scheme leads to a formally similar exponential expansion for the self-energies, and hence for the resulting HEOM, as compared with the widely used Matsubara expansion scheme. However, numerical tests have confirmed that with same N_p, the PFD scheme yields much more accurate approximation for $f_\alpha^{\mathfrak{s}}(z)$ than the Matsubara expansion scheme.[46,47] In other words, to achieve the same level of accuracy for the self-energies, a much smaller number of exponential terms is required with the PFD scheme. Therefore, the PFD scheme is superior to the conventional Matsubara expansion scheme in terms of computational efficiency.

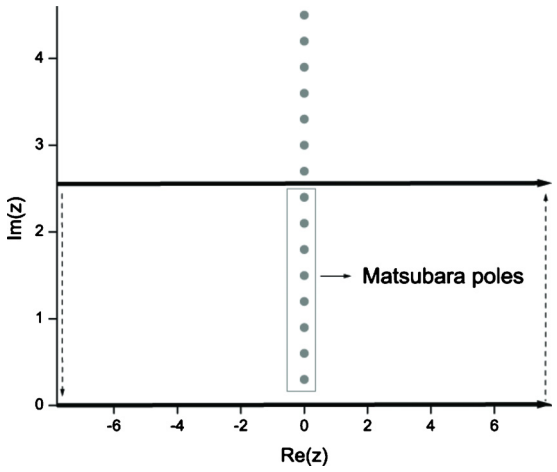

FIG. 1. An illustrative plot showing the contour of integration for $f_\alpha(z)\Lambda_\alpha(z)$ with a single-Lorentzian spectral density of $\Omega_1=5$. The dots equidistantly distributing on $\mathrm{Re}(z)=0$ correspond to the Matsubara poles (grey dots) in the upper complex plane. Integration along the dark solid arrow lying right on the real axis gives the desired self-energy of Eq. (30). However, the resulting HEOM encounters numerical difficulties. Due to the fact that the two dark solid arrows form a closed loop (completed with the dark dashed arrows at infinitely distance carrying zero values), the self-energy can be obtained alternatively by summing up the residues at the poles within this loop.

3. Hybrid spectral decomposition and frequency dispersion scheme

As mentioned after Eq. (34), in principle, $N_p\to+\infty$ is required to achieve an exact expansion for the Fermi function, and hence for the self-energies. With a finite N_p, the deviation between the RHS of Eq. (32) and the exact function $f_\alpha^{\mathfrak{s}}(z)$ results in the following contribution to the self-energies:

$$\tilde{\mathbf{\Sigma}}_\alpha^{x,\mathrm{dev}}(\tau-t) = \mathfrak{s}_x i\int_{\mathrm{Im}(z)=y} e^{iz(t-\tau)} f_\alpha^{\mathfrak{s}_x}(z)\mathbf{\Lambda}_\alpha(z)dz, \tag{36}$$

for $t\geq\tau$, as shown in Fig. 1. Different from Eq. (30) where the integration is along the real axis, here the integration contour is a horizontal line: $\mathrm{Im}(z)=y>0$. The value of y is chosen so that the first upper-plane N_p Matsubara poles reside in the interstitial region bounded by $\mathrm{Im}(z)=0$ and $\mathrm{Im}(z)=y$, while all the other poles are located outside this area, i.e., $(2N_p-1)\pi/\beta<y<(2N_p+1)\pi/\beta$.

As long as the modulus of $\mathbf{\Lambda}_\alpha(z)$ remains sufficiently small along the line $\mathrm{Im}(z)=y$, Eq. (36) presents a complementary contribution to the RHS of Eq. (33). The integration in Eq. (36) is transformed into summation of discrete terms, following the frequency dispersion scheme introduced in Sec. III A, i.e., $\int_{\mathrm{Im}(z)=y} g(z)dz \to \sum_{q=1}^{N_q} w_q g(\epsilon_q+iy)$. We have thus

$$\tilde{\mathbf{\Sigma}}_{\alpha}^{x,\mathrm{dev}}(\tau-t) \simeq \sum_{q=1}^{N_q} \boldsymbol{K}_{\alpha q}^{x} e^{-\hat{\gamma}_{\alpha q}(t-\tau)}, \tag{37}$$

with

$$\begin{aligned} \boldsymbol{K}_{\alpha q}^{x} &= \varsigma_x i w_q f_{\alpha}^{\varsigma_x}(\epsilon_q + iy)\mathbf{\Lambda}_{\alpha}(\epsilon_q + iy), \\ \hat{\gamma}_{\alpha q} &= -i(\epsilon_q + iy) = y - i\epsilon_q. \end{aligned} \tag{38}$$

Therefore, overall $\tilde{\mathbf{\Sigma}}_{\alpha}^{x}(\tau-t)$ is given by combining the RHS of Eqs. (33) and (37). The total number of exponential functions is $N_k=N_d+N_p+N_q$. In practice, to make use of Eq. (37), one needs to assign an appropriate number of Matsubara terms, N_p. On one hand, a smaller N_p leads to fewer unknown variables of HEOM. On the other hand, a too small N_p (and hence a too small y) would cause severe convergence problem when solving the stationary solutions of HEOM. Therefore, the value of N_p should be chosen carefully for the balance between computational cost and numerical difficulty. Once the N_p and y are settled, efficient quadratures can then be adopted to optimize the frequency dispersion (the set $\{w_q, \epsilon_q\}$ with $q=1,\ldots,N_q$) for Eq. (36). Finally, all the N_d poles of $\mathbf{\Lambda}_{\alpha}(z)$ inside the region $0<\mathrm{Im}(z)<y$ are collected.

It is important to note the value of N_d depends on the mathematical form of basis functions, based on which $\mathbf{\Lambda}_{\alpha}(\epsilon)$ is expanded. The widely used multi-Lorentzian expansion has been adopted in Sec. III B 1; see Eq. (31). Each Lorentzian function gives a pole in the upper complex plane. One of the advantages of using a Lorentzian function $g_{\mathrm{L}}(\epsilon)$ is that the magnitude of its analytically continued counterpart, $|g_{\mathrm{L}}(z)|$, decays smoothly as $\mathrm{Im}(z)$ increases. Therefore, the deviation term, $\tilde{\mathbf{\Sigma}}_{\alpha}^{x,\mathrm{dev}}(\tau-t)$ of Eq. (36), becomes consistently less significant as more Matsubara poles are considered explicitly. Alternative basis functions can also be used. For instance, a Gaussian function is analytic, and does not have any pole on the entire complex plane. Therefore, for $\mathbf{\Lambda}_{\alpha}(\epsilon)$ fitted by a number of Gaussian functions, $N_d=0$, which reduces the number of unknown variables of HEOM. However, care must be taken when treating the "deviation" contribution, as some of the $\boldsymbol{K}_{\alpha q}^{x}$ may assume large values, due to the nontrivial value of complex Gaussian function at certain $z=\epsilon_q+iy$.

Numerical tests on model systems[32] have confirmed that as the temperature lowers, the total number of exponential functions needed to accurately resolve the self-energies in the hybrid scheme grows much slower than that in the Matsubara expansion scheme.

IV. APPROXIMATE SCHEMES FOR CALCULATION OF DISSIPATION FUNCTIONAL

A. Schemes based on wide-band limit approximation

Even with the sophisticated hybrid scheme for decomposition of self-energies, the exact HEOM approach for the reduced electronic dynamics can still be expensive. Efficient approximate schemes are thus required. For clarity, we will omit the spin index in the following derivations of approximate schemes.

1. TDDFT-NEGF-HEOM formalism under wide-band limit approximation

The wide-band limit (WBL) approximation involves the following assumptions for the electrodes: (i) their bandwidths are assumed to be infinitely large; and (ii) their linewidths are assumed to be energy-independent, i.e., $\mathbf{\Lambda}_{\alpha}(\epsilon) \approx \mathbf{\Lambda}_{\alpha}$. Denote $\tilde{\mathbf{\Lambda}}_{\alpha} \equiv \pi\mathbf{\Lambda}_{\alpha}$. From the definition of self-energies and the expansion of the Fermi function [Eq. (32) with $N_p \to +\infty$], one obtains for $t>\tau$

$$\begin{aligned} \mathbf{\Sigma}_{\alpha}^{<,>}(\tau,t) &\equiv \pm i e^{i\int_{\tau}^{t} dt_1 \Delta_{\alpha}(t_1)} \int d\epsilon f_{\alpha}^{\pm}(\epsilon) e^{i\epsilon(t-\tau)} \mathbf{\Lambda}_{\alpha}(\epsilon) \\ &= \pm i\delta(t-\tau)\tilde{\mathbf{\Lambda}}_{\alpha} + \frac{2}{\beta}\sum_{k=1} e^{i\int_{\tau}^{t} dt_1 z_{\alpha k}(t_1)} \tilde{\mathbf{\Lambda}}_{\alpha}, \end{aligned} \tag{39}$$

where $z_{\alpha k}(t)=z_{\alpha k}+\Delta_{\alpha}(t)$. The expansion of Fermi function thus leads to a sum of exponentials for the self-energies. We introduce *auxiliary self-energies* $\hat{\mathbf{\Sigma}}_{\alpha k}$ to account for the exponentials, i.e.,

$$\mathbf{\Sigma}_{\alpha}^{<,>}(\tau,t) = \pm i\delta(t-\tau)\tilde{\mathbf{\Lambda}}_{\alpha} + \sum_{k} \hat{\mathbf{\Sigma}}_{\alpha k}(\tau,t), \tag{40}$$

$$\hat{\mathbf{\Sigma}}_{\alpha k}(\tau,t) = \frac{2}{\beta} e^{i\int_{\tau}^{t} dt_1 z_{\alpha k}(t_1)} \tilde{\mathbf{\Lambda}}_{\alpha}. \tag{41}$$

It is implied that $\hat{\mathbf{\Sigma}}_{\alpha k}(t,t^+)=\frac{2}{\beta}\tilde{\mathbf{\Lambda}}_{\alpha}$. Next, we insert relation Eq. (40) into Eq. (18), and arrive at

$$\boldsymbol{\varphi}_{\alpha}(t) = i[\mathbf{1} - 2\boldsymbol{\sigma}_{\mathrm{D}}(t)]\tilde{\mathbf{\Lambda}}_{\alpha} + \sum_{k} \hat{\boldsymbol{\varphi}}_{\alpha k}(t), \tag{42}$$

with the *auxiliary current matrices* being as follows:

$$\begin{aligned} \hat{\boldsymbol{\varphi}}_{\alpha k}(t) &= -i\int_{-\infty}^{t} d\tau [\boldsymbol{G}_{\mathrm{D}}^{<}(t,\tau) - \boldsymbol{G}_{\mathrm{D}}^{>}(t,\tau)]\hat{\mathbf{\Sigma}}_{\alpha k}(\tau,t) \\ &= i\int_{-\infty}^{t} d\tau \boldsymbol{G}_{\mathrm{D}}^{r}(t,\tau)\hat{\mathbf{\Sigma}}_{\alpha k}(\tau,t). \end{aligned} \tag{43}$$

Under the WBL approximation, NEGF formalism gives

$$\boldsymbol{G}_{\mathrm{D}}^{r}(t,\tau) = -i\vartheta(t-\tau)\boldsymbol{W}_{\mathrm{D}}^{-}(t)\boldsymbol{W}_{\mathrm{D}}^{+}(\tau), \tag{44}$$

$$\boldsymbol{W}_{\mathrm{D}}^{\pm}(t) = \exp_{\pm}\left\{ \mp i\int_{0}^{t} dt_1 [\boldsymbol{h}_{\mathrm{D}}(t_1) - i\tilde{\mathbf{\Lambda}}] \right\}. \tag{45}$$

Here, we take the time from which the voltage emerges as $t_0=0$, i.e., $\Delta_{\alpha}(t\leq 0)=0$, and $\tilde{\mathbf{\Lambda}}=\Sigma_{\alpha}\tilde{\mathbf{\Lambda}}_{\alpha}$. Therefore, the EOM of $\hat{\boldsymbol{\varphi}}_{\alpha k}(t)$ can be established readily as follows:

$$\dot{\hat{\boldsymbol{\varphi}}}_{\alpha k}(t) = \frac{2}{\beta}\tilde{\mathbf{\Lambda}}_{\alpha} - i[\boldsymbol{h}_{\mathrm{D}}(t) - i\tilde{\mathbf{\Lambda}} - z_{\alpha k}(t)]\hat{\boldsymbol{\varphi}}_{\alpha k}(t). \tag{46}$$

The coupled equations of motion, Eqs. (5), (27), (42), and (46) can be solved together for a complete description of the nonequilibrium electronic dynamics of the device. Equation (46) is self-closed, which suggests that under the WBL approximation the TDDFT-HEOM automatically terminates at

first tier, instead of second-tier termination for the exact formalism. Thus the additional second-tier auxiliary matrices[10] are not needed with the WBL. A similar approach has been adopted by Croy and Saalmann.[46]

2. TDDFT-NEGF-EOM formalism under adiabatic wide-band limit approximation

We consider another approximate scheme for $\boldsymbol{Q}_\alpha(t)$ based on WBL approximation for electrodes, as well as an adiabatic approximation for memory effect. The scheme aims at simplifying the TDDFT-NEGF formulation for $\boldsymbol{Q}_\alpha(t)$; see Eq. (10). Due to the WBL approximation, the ground/equilibrium-state self-energies become simply

$$\tilde{\boldsymbol{\Sigma}}^a_\alpha(\tau,t) = i\delta(t-\tau)\tilde{\boldsymbol{\Lambda}}_\alpha, \tag{47}$$

$$\tilde{\boldsymbol{\Sigma}}^<_\alpha(\tau,t) = i\frac{1}{\pi}\left[\int_{-\infty}^{+\infty} f_\alpha(\epsilon)e^{i\epsilon(t-\tau)}d\epsilon\right]\tilde{\boldsymbol{\Lambda}}_\alpha. \tag{48}$$

By inserting Eqs. (47) and (48) into Eq. (10), the dissipation functional is formally simplified to be

$$\boldsymbol{Q}^{\mathrm{AWBL}}_\alpha(t) = \{\tilde{\boldsymbol{\Lambda}}_\alpha, \boldsymbol{\sigma}_{\mathrm{D}}\} + \boldsymbol{P}_\alpha(t) + [\boldsymbol{P}_\alpha(t)]^\dagger, \tag{49}$$

$$\boldsymbol{P}_\alpha(t) = -\int_{-\infty}^{+\infty} \boldsymbol{G}^r_{\mathrm{D}}(t,\tau)\boldsymbol{\Sigma}^<_\alpha(\tau,t)d\tau. \tag{50}$$

Before the external voltage is applied, the entire composite system is in its ground/equilibrium state. We have

$$\boldsymbol{P}_\alpha(t) = -\frac{i}{\pi}\boldsymbol{U}^+_\alpha(t)\left\{\int_{-\infty}^{+\infty} f_\alpha(\epsilon)\left[\frac{1}{\epsilon-\boldsymbol{h}_{\mathrm{D}}(0)+i\tilde{\boldsymbol{\Lambda}}} - i\int_0^t e^{-i\epsilon\tau}\boldsymbol{U}^-_\alpha(\tau)d\tau\right]e^{i\epsilon t}d\epsilon\right\}\tilde{\boldsymbol{\Lambda}}_\alpha. \tag{51}$$

$$\boldsymbol{U}^\pm_\alpha(t) \equiv \exp_\pm\left\{\mp i\int_0^t d\tau[\boldsymbol{h}_{\mathrm{D}}(\tau) - i\tilde{\boldsymbol{\Lambda}} - \Delta_\alpha(\tau)]\right\}. \tag{52}$$

To facilitate the calculation of $\boldsymbol{P}_\alpha(t)$ given by Eq. (51), an adiabatic approximation is adopt to evaluate the time integral within the square bracket on the RHS. The basic idea is to first disregard the time-dependence of $\boldsymbol{h}_{\mathrm{D}}(t)$ and $\Delta_\alpha(t)$ in Eq. (52), evaluate the time integral, and then restore subsequently the time-dependence of $\boldsymbol{h}_{\mathrm{D}}(t)$ and $\Delta_\alpha(t)$. The final approximated expression for $\boldsymbol{P}_\alpha(t)$ is as follows:

$$\boldsymbol{P}_\alpha(t) \simeq -\frac{i}{\pi}\left\{\boldsymbol{U}^+_\alpha(t)\int_{-\infty}^{+\infty} d\epsilon f_\alpha(\epsilon)e^{i\epsilon t}\times\left[\frac{1}{\epsilon-\boldsymbol{h}_{\mathrm{D}}(0)+i\tilde{\boldsymbol{\Lambda}}} - \frac{1}{\epsilon-\boldsymbol{h}_{\mathrm{D}}(t)+i\tilde{\boldsymbol{\Lambda}}+\Delta_\alpha(t)}\right] + \int_{-\infty}^{+\infty}\frac{f_\alpha(\epsilon)}{\epsilon-\boldsymbol{h}_{\mathrm{D}}(t)+i\tilde{\boldsymbol{\Lambda}}+\Delta_\alpha(t)}d\epsilon\right\}\tilde{\boldsymbol{\Lambda}}_\alpha. \tag{53}$$

The RHS of Eq. (53) gives exact $\boldsymbol{P}_\alpha(t)$ for the ground state at $t\le 0$ and the steady state at $t\to+\infty$, provided that $\Delta_\alpha(t\to+\infty)$ is a constant. At $0<t<+\infty$, it provides an adiabatic connection between the ground and steady states. Equation (53) can be solved conveniently, along with the EOM for $\boldsymbol{U}^+_\alpha(t)$ as follows:

$$i\dot{\boldsymbol{U}}^+_\alpha(t) = [\boldsymbol{h}_{\mathrm{D}}(t) - i\tilde{\boldsymbol{\Lambda}} - \Delta_\alpha(t)]\boldsymbol{U}^+_\alpha(t). \tag{54}$$

B. Scheme based on complete second-order quantum dissipation theory

As presented in Sec. III, the TDDFT-NEGF-HEOM for KS RSDM and associated auxiliary matrices terminate exactly at the second tier. This amounts to an explicit treatment of device-electrode interaction at leading fourth-order.[10] The number of unknown matrices at zeroth, first, and second tier is 1, $N_\alpha N_k$, and $N^2_\alpha N^2_k$, respectively. Here, N_k is the number of exponential functions used to resolve the memory contents of self-energies or electrode correlation functions. Obviously, the second-tier variables dominate the computational cost for solving the TDDFT-NEGF-HEOM. Therefore, a straightforward way to reduce the computational expense is to avoid explicit involvement of the second-tier variables, i.e., to truncate the TDDFT-NEGF-HEOM at first tier approximately.

A simple truncation scheme is to set all second-tier auxiliary matrices to zero, i.e., $\boldsymbol{\varphi}_{\alpha k,\alpha' k'}(t)=\boldsymbol{0}$. This corresponds to the chronological ordering prescription of second-order QDT. An alternative second-order approximation is as follows:

$$\boldsymbol{G}^<_{\mathrm{D}}(t,\tau) \approx i\boldsymbol{\sigma}_{\mathrm{D}}(t)\boldsymbol{U}^+_{\mathrm{D}}(t,\tau), \qquad \boldsymbol{G}^>_{\mathrm{D}}(t,\tau) \approx -i\bar{\boldsymbol{\sigma}}_{\mathrm{D}}(t)\boldsymbol{U}^+_{\mathrm{D}}(t,\tau), \tag{55}$$

with

$$\boldsymbol{U}^\pm_{\mathrm{D}}(t,\tau) = \exp_\pm\left[\mp i\int_\tau^t \boldsymbol{h}_{\mathrm{D}}(\zeta)d\zeta\right]. \tag{56}$$

The dissipation functional becomes approximately

$$\boldsymbol{Q}_\alpha(t) \approx [\boldsymbol{\sigma}_{\mathrm{D}}(t)\boldsymbol{\Pi}^>_\alpha(t) + \bar{\boldsymbol{\sigma}}_{\mathrm{D}}(t)\boldsymbol{\Pi}^<_\alpha(t) + \mathrm{H.c.}], \tag{57}$$

where

$$\boldsymbol{\Pi}^x_\alpha(t) = i\int_{-\infty}^t d\tau\boldsymbol{U}^+_{\mathrm{D}}(t,\tau)\boldsymbol{\Sigma}^x_\alpha(\tau,t). \tag{58}$$

Following Sec. III, we decompose self-energies as linear combinations of exponential functions; see Eq. (26). This leads to

$$\boldsymbol{\Pi}^x_\alpha(t) = \sum_{k=1}^{N_k}\boldsymbol{\Pi}^x_{\alpha k}(t), \qquad \boldsymbol{\Pi}^x_{\alpha k}(t) = i\int_{-\infty}^t d\tau\boldsymbol{U}^+_{\mathrm{D}}(t,\tau)\tilde{\boldsymbol{\Sigma}}^x_{\alpha k}(\tau-t)e^{i\int_\tau^t\Delta_\alpha(\zeta)d\zeta}. \tag{59}$$

The EOM for $\boldsymbol{\Pi}^x_{\alpha k}(t)$ is thus

$$i\dot{\boldsymbol{\Pi}}^x_{\alpha k}(t) = [\boldsymbol{h}_{\mathrm{D}}(t) - i\gamma_{\alpha k} - \Delta_\alpha(t)]\boldsymbol{\Pi}^x_{\alpha k}(t) - \boldsymbol{A}^x_{\alpha k}, \tag{60}$$

with $\boldsymbol{A}^x_{\alpha k}$ and $\gamma_{\alpha k}$ referring to Eq. (26).

The resulting complete second-order QDT approach thus involves the coupled EOM for $\boldsymbol{\sigma}_{\mathrm{D}}(t)$ and $\{\boldsymbol{\Pi}^x_{\alpha k}(t)\}$, with the

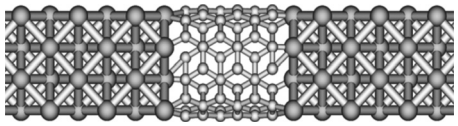

FIG. 2. The ball-and-stick representation of the system of interest which is a carbon nanotube (5,5) welded to aluminum electrodes. There are 60 carbon atoms for the carbon nanotube in this case.

total number of unknown matrices being $N=2N_\alpha N_k+1$, much fewer than $N_\alpha^2 N_k^2$ alone. This approach can be improved further, by formal inclusion of higher-order device-electrode interaction into the reduced system propagator $\boldsymbol{U}_{\mathrm{D}}^{+}(t,\tau)$. This can be achieved by attaching self-energy to $\boldsymbol{h}_{\mathrm{D}}(t)$ on the RHS of Eq. (56).

V. NUMERICAL RESULTS

As a test for our practical schemes, we have performed numerical calculations by employing the ALDA approximation for the XC potential and AWBL approximation for the dissipation functional. The latter has been outlined in Sec. IV A 2. LODESTAR (Ref. 48) was used to carry out the calculations. The system of interest is a (5,5) carbon nanotube which is covalently bonded between two aluminum electrodes, as shown in Fig. 2. In the simulation box, we include a finite carbon nanotube and 32 aluminum atoms for each electrode explicitly. The minimum basis set STO-3G is adopted in the calculations. We simulate the time-dependent electric current through the left (right) electrode by taking the trace of the corresponding dissipative term $\boldsymbol{Q}_{\mathrm{L}}$ ($\boldsymbol{Q}_{\mathrm{R}}$); see Eq. (8).

Figure 3 shows the currents versus time for different numbers of carbon atoms, i.e., 20, 40, 60, and 80. The bias voltage V_b is switched on exponentially at $t=0$ and as shown in Fig. 3. We observe that the currents reach their steady states in about 8–12 fs for different systems. Also, the value of the steady state current does not increase proportionally with the size of the carbon nanotube, as that of classical case. We note from Fig. 3 that the steady state currents for the systems with 20, 40, 60, and 80 carbon atoms are about 21, 9, 14, and 4 μA, respectively. This shows that the quantum finite size effect plays an important role at such small scales. We point out that all the above calculations are performed on single-CPU desktop personal computer, and the memory is 2 Gbytes.

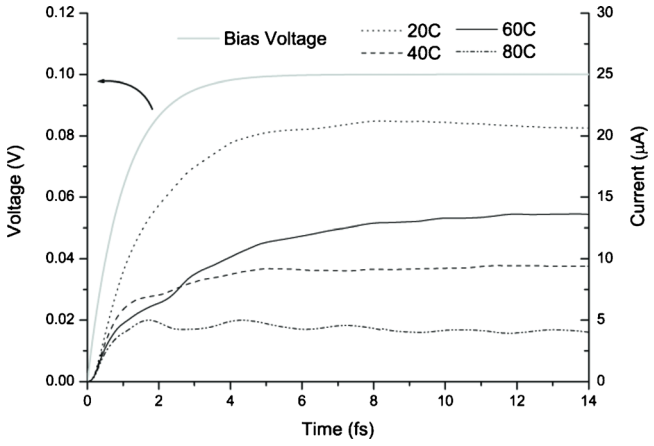

FIG. 3. The grey solid line represents the bias voltage applied on the systems. The bias voltage is switched on exponentially, $V_b=V_0(1-e^{-t/a})$ with $V_0=0.1$ V and time constant $a=1$ fs. The transient currents for the systems with 20, 40, 60, and 80 carbon atoms are shown dark dotted line, dashed line, solid line, and dashed-dot-dot line respectively.

VI. CONCLUDING REMARKS

We have proposed a first-principles TDDFT-NEGF-HEOM method for transient quantum transport through realistic electronic devices and structures. The TDDFT-NEGF-HEOM formalism is, in principle, exact and formally equivalent to the TDDFT-NEGF-EOM formalism proposed previously. In practice, it involves hierarchical equations for KS RSDM of reduced system and associated auxiliary quantities.

By resolving memory contents of self-energies or electrode correlation functions, we construct QDT-HEOM in the KS reduced single-electron space. The resulting TDDFT-HEOM exactly terminate at the second tier. TDDFT-NEGF-HEOM formalism combines TDDFT-NEGF-EOM and TDDFT-HEOM, and its computational cost is determined by the number of exponential functions used to expand the self-energies. Various decomposition schemes are presented.

To reduce computational cost further, we have also devised approximate schemes for TDDFT-NEGF-HEOM. One is based on the WBL treatment for self-energies. Another one is based on complete second-order QDT. These approximate schemes significantly reduce the computational cost, and improve the efficiency for solving the reduced electronic dynamics. Additional adiabatic approximation is introduced for the WBL scheme, and the resulting AWBL approximation turns out the most efficient scheme. Numerical simulations based on the AWBL scheme demonstrate that first-principles simulation can indeed be carried out for real devices, and the interesting results have been obtained.

ACKNOWLEDGMENTS

Support from the Hong Kong Research Grant Council (Contract Nos. HKU7009/09P, 7008/08P, 7011/06P, 7013/07P, 604709, and HKUST 9/CRF/08), the University Grant Council (Contract No. AoE/P-04/08) and National Science Foundation of China (Contract No. NSFC 20828003) is gratefully acknowledged.

[1] E. Runge and E. K. U. Gross, Phys. Rev. Lett. **52**, 997 (1984).
[2] G. Stefanucci and C.-O. Almbladh, Europhys. Lett. **67**, 14 (2004); Phys. Rev. B **69**, 195318 (2004).
[3] S. Kurth, G. Stefanucci, C.-O. Almbladh, A. Rubio, and E. K. U. Gross, Phys. Rev. B **72**, 035308 (2005).
[4] X. Zheng and G. H. Chen, e-print arXiv:physics/0502021; C. Y. Yam, X. Zheng, and G. H. Chen, J. Comput. Theor. Nanosci. **3**, 857 (2006).
[5] X. Zheng, F. Wang, and G. H. Chen, arXiv:quant-ph/0606169; G. H. Chen, in *Recent Progress in Computational Sciences and Engineering*, Lecture Series on Computer and Computational Sciences Vol. 7, edited by T. Simos and G. Maroulis (Brill, Leiden, 2006), p. 803.
[6] X. Zheng, F. Wang, C. Y. Yam, Y. Mo, and G. H. Chen, Phys. Rev. B **75**, 195127 (2007).
[7] C. Y. Yam, Y. Mo, F. Wang, X. B. Li, G. H. Chen, X. Zheng, Y. Matsuda, J. Tahir-Kheli, and W. A. Goddard III, Nanotechnology **19**, 495203 (2008).
[8] P. Cui, X. Q. Li, J. Shao, and Y. J. Yan, Phys. Lett. A **357**, 449 (2006); X.

Q. Li and Y. J. Yan, Phys. Rev. B **75**, 075114 (2007).
[9] K. Burke, R. Car, and R. Gebauer, Phys. Rev. Lett. **94**, 146803 (2005).
[10] J. S. Jin, X. Zheng, and Y. J. Yan, J. Chem. Phys. **128**, 234703 (2008).
[11] A. Nakano, P. Vashishta, and R. K. Kalia, Phys. Rev. B **43**, 9066 (1991).
[12] C.-L. Cheng, J. S. Evans, and T. Van Voorhis, Phys. Rev. B **74**, 155112 (2006).
[13] N. Sai, N. Bushong, R. Hatcher, and M. Di Ventra, Phys. Rev. B **75**, 115410 (2007).
[14] S. Yokojima and G. H. Chen, Chem. Phys. Lett. **292**, 379 (1998); Phys. Rev. B **59**, 7259 (1999); Chem. Phys. Lett. **300**, 540 (1999); S. Yokojima, D. H. Zhou, and G. H. Chen, *ibid.* **302**, 495 (1999); W. Z. Liang, S. Yokojima, D. H. Zhou, and G. H. Chen, J. Phys. Chem. A **104**, 2445 (2000); W. Z. Liang, S. Yokojima, and G. H. Chen, J. Chem. Phys. **110**, 1844 (1999); W. Z. Liang, S. Yokojima, M. F. Ng, G. H. Chen, and G. He, J. Am. Chem. Soc. **123**, 9830 (2001).
[15] C. Y. Yam, S. Yokojima, and G. H. Chen, Phys. Rev. B **68**, 153105 (2003); J. Chem. Phys. **119**, 8794 (2003); F. Wang, C. Y. Yam, G. H. Chen, and K. N. Fan, *ibid.* **126**, 134104 (2007).
[16] Y. Mo, X. Zheng, G. H. Chen, and Y. J. Yan, J. Phys.: Condens. Matter **21**, 355301 (2009).
[17] W. Kohn and L. J. Sham, Phys. Rev. **140**, A1133 (1965).
[18] N. Sai, M. Zwolak, G. Vignale, and M. Di Ventra, Phys. Rev. Lett. **94**, 186810 (2005).
[19] F. Rossi, A. Di Carlo, and P. Lugli, Phys. Rev. Lett. **80**, 3348 (1998).
[20] S. Weiss, J. Eckel, M. Thorwart, and R. Egger, Phys. Rev. B **77**, 195316 (2008).
[21] P. Myöhänen, A. Stan, G. Stefanucci, and R. van Leeuwen, EPL **84**, 67001 (2008); Phys. Rev. B **80**, 115107 (2009).
[22] L. P. Kadanoff and G. Baym, *Quantum Statistical Mechanics* (Benjamin, New York, 1962).
[23] N. E. Dahlen and R. van Leeuwen, Phys. Rev. Lett. **98**, 153004 (2007).
[24] U. Harbola, M. Esposito, and S. Mukamel, Phys. Rev. B **74**, 235309 (2006).
[25] U. Harbola and S. Mukamel, in *Theory and Applications of Computational Chemistry: The First Forty Years*, edited by C. E. Dykstra, G. Frenking, K. S. Kim, and G. E. Scuseria (Elsevier, Amsterdam, 2005), pp. 373–396.
[26] G. Q. Li, S. Welack, M. Schreiber, and U. Kleinekathöfer, Phys. Rev. B **77**, 075321 (2008).
[27] S. Welack, S. Mukamel, and Y. J. Yan, EPL **85**, 57008 (2009).
[28] J. S. Jin, S. Welack, J. Y. Luo, X. Q. Li, P. Cui, R. X. Xu, and Y. J. Yan, J. Chem. Phys. **126**, 134113 (2007).
[29] X. Zheng, J. S. Jin, and Y. J. Yan, J. Chem. Phys. **129**, 184112 (2008).
[30] X. Zheng, J. S. Jin, and Y. J. Yan, New J. Phys. **10**, 093016 (2008).
[31] X. Zheng, J. Y. Luo, J. S. Jin, and Y. J. Yan, J. Chem. Phys. **130**, 124508 (2009).
[32] X. Zheng, J. S. Jin, S. Welack, M. Luo, and Y. J. Yan, J. Chem. Phys. **130**, 164708 (2009).
[33] M. E. Casida, *Recent Developments and Applications in Density Functional Theory* (Elsevier, Amsterdam, 1996).
[34] S. Fournais, M. Hoffmann-Ostenhof, T. Hoffmann-Ostenhof, and T. Ø. Sørensen, Ark. Mat. **42**, 87 (2004).
[35] J. Riess and W. Münch, Theor. Chim. Acta **58**, 295 (1981).
[36] P. G. Mezey, Mol. Phys. **96**, 169 (1999).
[37] S. K. Ghosh and A. K. Dhara, Phys. Rev. A **38**, 1149 (1988).
[38] G. Vignale and W. Kohn, Phys. Rev. Lett. **77**, 2037 (1996).
[39] M. Di Ventra and R. D'Agosta, Phys. Rev. Lett. **98**, 226403 (2007).
[40] G. Vignale, Phys. Rev. A **77**, 062511 (2008).
[41] R. van Leeuwen, Phys. Rev. Lett. **80**, 1280 (1998).
[42] S. Mukamel, Phys. Rev. A **71**, 024503 (2005).
[43] M. Cini, Phys. Rev. B **22**, 5887 (1980).
[44] C. Caroli, R. Combescot, P. Nozìeres, and D. Saint-James, J. Phys. C **4**, 916 (1971); C. Caroli, R. Combescot, D. Lederer, P. Nozìeres, and D. Saint-James, J. Phys. C **4**, 2598 (1971).
[45] See supplementary material at http://dx.doi.org/10.1063/1.3475566 for detailed derivation of HEOM for an open noninteracting system (Sec. I), for details and remarks on Landauer–Büttiker formula for steady current (Sec. II), and for expression of the self-energy.
[46] A. Croy and U. Saalmann, Phys. Rev. B **80**, 245311 (2009).
[47] J. Xu, R. X. Xu, M. Luo, and Y. J. Yan, Chem. Phys. **370**, 109 (2010).
[48] G. H. Chen, C. Y. Yam, S. Yokojima, W. Z. Liang, X. J. Wang, F. Wang, and X. Zheng, http://yangtze.hku.hk/LODESTAR/lodestar.php.